

Structure and Dynamics of Glyceride Lipid Formulations, with Propylene Glycol and Water

Dallas B. Warren, David K. Chalmers, and Colin W. Pouton*

*Medicinal Chemistry and Drug Action, Monash Institute of Pharmaceutical Sciences,
Monash University (Parkville Campus), Melbourne, Victoria, Australia*

Received September 15, 2008; Revised Manuscript Received January 15, 2009; Accepted
March 4, 2009

Abstract: We report on the aggregation and dynamic behavior of excipients in type I and surfactant-free lipid formulations containing water-soluble cosolvents. Specifically we have investigated the internal structure of mixed glyceride formulations, with and without propylene glycol, in the anhydrous state and during dilution into water. We performed molecular dynamics (MD) simulations using GROMACS 3.1.4 (www.gromacs.org) to investigate the aggregation structures and phase changes which would occur on dispersion and dilution of the product in the gastrointestinal tract. MD experiments on mixed glyceride lipid formulations, revealed that they form microstructural features even in the presence of trace amounts of water, typical of what would be anticipated in capsule formulations in practice. These formulations are typically thought of as homogeneous mixtures, a view which has prevailed to some extent because the chemical diversity (chain length and degree of saturation) in excipients derived from vegetable oils prevents analysis of their microstructure by spectroscopic techniques. Our MD simulations suggest that a considerable depth of structure exists in the formulations, and that drugs partition into the various domains under the influence of intermolecular interactions, often dominated in the presence of water by hydrogen bonding. The lipid formulations consist of distinct regions of hydrophobic and hydrophilic character, essentially exhibiting reverse micellar character under low-water-content conditions. MD modeling has great potential as a predictive tool, in particular to identify drugs which may be prone to precipitation on dilution or dispersion of the lipid formulation.

Keywords: Molecular dynamics; mixed mono- and diglycerides; propylene glycol; lipid formulations; reverse micelle structure; microemulsion; spontaneous structuring; drug microenvironment

Introduction

Lipid formulations are of increasing importance for the oral administration of drugs,¹ particularly since a growing proportion of drug candidates are very poorly soluble in

water.² A variety of excipients can be included in lipid formulations. Their performance depends on the fate of the drug after initial dispersion of the product, most likely in the stomach after release from a hard or soft-gelatin capsule, and after exposure of the product to the powerful digestive system of the small intestine. The factors affecting absorption of drugs from lipid systems are not sufficiently well-defined to facilitate predictive modeling of *in vivo* performance from

* Author to whom correspondence should be addressed. Mailing address: Medicinal Chemistry and Drug Action, Monash Institute of Pharmaceutical Sciences, Monash University (Parkville Campus), Melbourne, Victoria, Australia. Phone: +61 3 9903 9562. Fax: +61 3 9903 9638. E-mail: colin.pouton@pharm.monash.edu.au.

(1) Humberstone, A. J.; Charman, W. N. Lipid-based vehicles for the oral delivery of poorly water soluble drugs. *Adv. Drug Delivery Rev.* **1997**, *25*, 103–128.

(2) Lipinski, C. A. Drug-like properties and the causes of poor solubility and poor permeability. *J. Pharmacol. Toxicol. Methods* **2000**, *44*, 235–249.

(3) Reymond, J. P.; Sucker, H. In vitro model for ciclosporin intestinal absorption in lipid vehicles. *Pharm. Rev.* **1988**, *5*, 673–676.

in vitro tests, but *in vitro* lipolysis tests are emerging,^{3–7} and a lipid formulation classification system (LFCS) has been introduced that will help anticipation of *in vivo* performance.^{8,9}

The general objective of a lipid formulation is to present the drug to the gut in solution, thereby avoiding the slow dissolution of hydrophobic drugs from the crystalline form. An additional requirement for efficient absorption is that the oily solution becomes dispersed in the intestine as a colloidal system, either by self-dispersion or as a result of digestion of the glyceride components by pancreatic lipase (or both). During these dispersion and/or digestion processes the solvent properties and solvent capacity of the formulation may change, which can lead to precipitation of the drug, in which case the advantage of the lipid formulation may well be lost. Recent bioavailability studies in our laboratories have demonstrated this issue clearly with the drug danazol. The bioavailability of danazol was reduced when dogs were given formulations from which the drug was known to precipitate in *in vitro* lipolysis assays.¹⁰

Molecular dynamics (MD) simulations are a powerful technique to investigate aggregates on the molecular scale and have not been performed on lipid formulations to date. MD has provided useful insight into the structure and dynamics of micelles, including model,^{11–13} cationic,^{14,15}

glycoside,¹⁶ sodium dodecyl sulfate (SDS),^{17,18} phospholipid^{19,20} and bile salt/phospholipid²¹ systems. To increase the speed of calculations and allow access to large simulation system sizes within a reasonable time, united atom forcefields have been extensively used. Simulations of salt/phospholipid micelles,²¹ simple surfactant micelles,^{18,22} and bilayers^{22–26} using united atom forcefields successfully reproduce experimental results of interest to this study: the formation and structure of micelles.

In the present study we have investigated the internal structure of type I lipid formulations containing mixed glycerides using molecular dynamics simulations. We first investigated the formulations in anhydrous form and in the presence of trace amounts of water, which we suggest represents the expected water-content of a blend of glyceride excipients in a soft-gelatin capsule. Subsequently we inves-

-
- (4) MacGregor, K. J.; Embleton, J. K.; Lacy, J. E.; Perry, E. A.; Solomon, L. J.; Seager, H.; Pouton, C. W. Influence of lipolysis on drug absorption from the gastro-intestinal tract. *Adv. Drug Delivery Rev.* **1997**, *25*, 33–46.
- (5) Porter, C. J. H.; Charman, W. N. In vitro assessment of oral lipid based formulations. *Adv. Drug Delivery Rev.* **2001**, *50*, S127–S147.
- (6) Zangenberg, N. H.; Mullertz, A.; Kristensen, H. G.; Hovgaard, L. A dynamic in vitro lipolysis model. i. controlling the rate of lipolysis by continuous addition of calcium. *Eur. J. Pharm. Sci.* **2001**, *14*, 115–122.
- (7) Kaukonen, A. M.; Boyd, B. J.; Porter, C. J.; Charman, W. N. Drug solubilization behavior during in vitro digestion of simple triglyceride lipid solution formulations. *Pharm. Res.* **2004**, *21*, 245–253.
- (8) Pouton, C. W. Lipid formulations for oral administration of drugs: non-emulsifying, self-emulsifying and ‘self-microemulsifying’ drug delivery systems. *Eur. J. Pharm. Sci.* **2000**, *11*, S93–S98.
- (9) Pouton, C. W. Formulation of poorly water-soluble drugs for oral administration: physicochemical and physiological issues and the lipid formulation classification system. *Eur. J. Pharm. Sci.* **2006**, *29*, 278–287.
- (10) Cuine, J. F.; Charman, W. N.; Pouton, C. W.; Edwards, G. A.; Porter, C. J. Increasing the proportional content of surfactant (cremophor el) relative to lipid in self-emulsifying lipid-based formulations of danazol reduces oral bioavailability in beagle dogs. *Pharm. Res.* **2007**, *24*, 748–757.
- (11) Gruen, D. W. R. A model for the chains in amphiphilic aggregates: I comparison with a molecular dynamics simulation of a bilayer. *J. Phys. Chem.* **1985**, *89*, 146–153.
- (12) Abu-Sharkh, B. F.; Hamad, E. Z. Investigation of the microstructure of micelles formed by hard-sphere chains interacting via size nonadditivity by discontinuous molecular dynamics simulation. *Langmuir* **2004**, *20*, 254–259.
- (13) Woods, M. C.; Haile, J. M.; O’Connell, J. P. Internal structure of a model micelle via computer simulation: 2 spherical confined aggregates with mobile head groups. *J. Phys. Chem.* **1986**, *90*, 1875–1885.
- (14) Maillet, J.; Lachet, V.; Coveney, P. V. Large scale molecular dynamics simulation of self-assembly processes in short and long chain cationic surfactants. *Phys. Chem. Chem. Phys.* **1999**, *1*, 5277–5290.
- (15) Shinto, H.; Morisada, S.; Miyahara, M.; Higashitani, K. Langevin dynamics simulations of cationic surfactants in aqueous solutions using potentials of mean force. *Langmuir* **2004**, *20*, 2017–2025.
- (16) Bogusz, S.; Venable, R. M.; Pastor, R. W. Molecular dynamics simulations of octyl glucoside micelles: structural properties. *J. Phys. Chem. B* **2000**, *104*, 5462–5470.
- (17) Bruce, C. D.; Berkowitz, M. L.; Perera, L.; Forbes, M. D. E. Structural characteristics and counterion distribution. *J. Phys. Chem. B* **2002**, *106*, 3788–3793.
- (18) Rakitin, A. R.; Pack, G. R. Molecular dynamics simulations of ionic interactions with dodecyl sulfate micelles. *J. Phys. Chem. B* **2004**, *108*, 2712–2716.
- (19) Tieleman, D. P.; van der Spoel, D.; Berendsen, H. J. C. Molecular dynamics simulations of dodecylphosphocholine micelles at three different aggregate sizes: micellar structure and chain relaxation. *J. Phys. Chem. B* **2000**, *104*, 6380–6388.
- (20) Marrink, S. J.; Mark, A. E. Molecular dynamics simulation of the formation, structure, and dynamics of small phospholipid vesicles. *J. Am. Chem. Soc.* **2003**, *125*, 15233–15242.
- (21) Marrink, S. J.; Mark, A. E. Molecular dynamics simulations of mixed micelles modelling human bile. *Biochemistry* **2002**, *41*, 5375–5382.
- (22) Schuler, L. D.; Walde, P.; Luisi, P. L.; van Gunsteren, W. F. Molecular dynamics simulation of *n*-dodecyl phosphate aggregate structures. *Eur. J. Biochem.* **2001**, *30*, 330–343.
- (23) Chiu, S. W.; Jakobsson, E.; Mashl, R. J.; Scott, H. L. Cholesterol-induced modifications in lipid bilayers: a simulation study. *Biophys. J.* **2002**, *83*, 1842–1853.
- (24) Lindahl, E.; Edholm, O. Molecular dynamics simulation of NMR relaxation rates and slow dynamics in lipid bilayers. *J. Chem. Phys.* **2001**, *115*, 4938–4950.
- (25) Bachar, M.; Brunelle, P.; Tieleman, D. P.; Rauk, A. Molecular dynamics simulation of a polyunsaturated lipid bilayer susceptible to lipid peroxidation. *J. Phys. Chem. B* **2004**, *108*, 7170–7179.
- (26) Smondyrev, A. M.; Berkowitz, M. L. Molecular dynamics simulation of the structure of dimyristoylphosphatidylcholine bilayers with cholesterol, ergosterol, and lanosterol. *Biophys. J.* **2001**, *80*, 1649–1658.

tigated the structure of systems containing increasing proportions of water, to give an indication of how the structure changes during dispersion of the formulation in the aqueous contents of the gastrointestinal tract. Specifically, we report MD simulations of the spontaneous structuring behavior of monolauryl glyceride (MGL) and dilauryl glyceride (DGL) in the presence of water and/or propylene glycol (PG).

Experimental Section

Software and Hardware. The GROMACS^{27–29} software package (www.gromacs.org) was used to perform the MD simulations. Full specifications of the computer systems utilized are in a previous paper.³⁰ Visualization of the simulation trajectories was performed using the software package VMD.³¹ Subsequent analysis scripts were all packaged with GROMACS. The spatial distribution function of atoms relative to the molecules was generated using `g_sdf`³² (bin width = 0.09 nm), version 1.25. The radial distribution function between selected atoms was calculated using `g_rdf` (bin width = 0.001 nm), integrated across the hydration shell volumes to obtain the water coordination number for each shell and then divided by the water coordination number for a single molecule simulated within water only. The self-diffusion coefficient was calculated with `g_msd`. `g_msd` calculates the mean square displacement of atoms/molecules from their initial positions, fits a straight line using the least-squares method to the mean square displacement and computes the self-diffusion constant using the Einstein relation.

Simulation Specifications. The 43a2 united atom (CH, CH₂ and CH₃ groups represented as a single “atom”) forcefield, one of the GROMOS-96 force fields,³³ was used for the molecular dynamic simulations. Rigid SPC water³⁴

was the water model used and was constrained using SETTLE.³⁵ Remaining solute bonds were constrained by the LINCS algorithm,³⁶ and temperature and pressure control was executed by Berendsen coupling.³⁷ Periodic boundary conditions were employed on the cubic simulation box, along with a cutoff distance of 1.5 nm for electrostatic and 1.0 nm for Lennard-Jones nonbonding interactions. To achieve a large simulation time step, the fastest vibrational frequency within the bile salt molecules, exhibited by the polar hydrogens, was reduced by increasing the mass of the hydrogen atom to 4 Da. The attached heavy atom’s mass was decreased by the same amount to conserve mass.³⁸ This mass redistribution was only applied to the polar hydrogens within the bile salt molecules and allowed the use of a 5 fs time step, with such large time steps being used increasingly in simulations.^{19,21,39–42}

All of the MD simulations were established and performed using the following procedure. Each of the appropriate glyceride molecules were randomly distributed in turn within a cubic simulation box. The box was then solvated with the appropriate number of propylene glycol and/or water molecules. Steepest descent energy minimization²⁹ was used to remove bad van der Waals contacts between atoms. This was followed by two short 20 and 40 ps simulations to allow initial stabilization of the system. The first short simulation was performed with temperature ($\tau_T = 0.01$ ps with reference temperature of 310 K) and no pressure coupling, the second with temperature ($\tau_T = 0.1$ ps) and anisotropic pressure ($\tau_P = 4.0$ ps with reference pressure of 1 bar and 4.5×10^{-5} compressibility in the x , y and z directions) coupling. From these second trajectory and coordinate files the production MD simulations was commenced. The production simulations used a time step of 5 fs, anisotropic coupling with $P_{\text{ref}} = 1$ atm, $\tau_P = 1$ ps, and temperature coupling with $T_{\text{ref}} = 310$ K, $\tau_T = 0.05$ ps. The bulk system properties reached stable levels after a maximum of 5 ns and then oscillated

- (27) Lindahl, E.; Hess, B.; van der Spoel, D. GROMACS 3.0: a package for molecular simulation and trajectory analysis. *J. Mol. Modelling* **2001**, *7*, 306–317.
- (28) Berendsen, H. J. C.; van der Spoel, D.; van Drunen, R. GROMACS: a message-passing parallel molecular dynamics implementation. *Comput. Phys. Commun.* **1995**, *91*, 43–56.
- (29) van der Spoel, D.; van Buuren, A. R.; Apol, E.; Meulenhoff, P. J.; Tieleman, D. P.; Sijbers, A.L.T.M.; Hess, B.; Feenstra, K. A.; Lindahl, E.; van Drunen, R.; Berendsen, H. J. C. *GROMACS user manual version 3.1.1*, 3.1.1 ed.; Department of Biophysical Chemistry: Groningen, 2002.
- (30) Warren, D. B.; Chalmers, D. K.; Hutchison, K.; Dang, W.; Pouton, C. W. Molecular dynamics simulation of spontaneous bile salt aggregation. *Colloids Surf., A* **2006**, *280*, 182–193.
- (31) Humphrey, W.; Dalke, A.; Schulten, K. Vmd: visual molecular dynamics. *J. Mol. Graphics* **1996**, *14*, 33–38.
- (32) Freudenberger, C., `G_sdf`, 1.25, Chemistry, University of Ulm, 2003.
- (33) van Gunsteren, W. F.; Billeter, S. R.; Eising, A. A.; Hunenberger, P. H.; Krueger, P.; Mark, A. E.; Scott, W. R. P.; Tironi, I. G. *Biomolecular simulation: the GROMOS96 manual and user guide*, 1st ed.; Hochschulverlag AG an der ETHC Zurich: Zurich, 1996.
- (34) Berendsen, H. J. C.; Postma, J. P. M.; van Gunsteren, W. F.; Hermans, J.; Pullman, B. Interaction models for water in relation to protein hydration. In *Intermolecular forces*; Pullman, B., Ed.; D. Reidel Publishing Company: Dordrecht, 1981; pp 331–342.

- (35) Miyamoto, S.; Kollman, P. A. SETTLE: an analytical version of the shake and rattle algorithm for rigid water models. *J. Comput. Chem.* **1992**, *13*, 952–962.
- (36) Hess, B.; Bekker, H.; Berendsen, H. J. C.; Fraaije, J.G.E.M. LINCS: a linear constraint solver for molecular simulations. *J. Comput. Chem.* **1997**, *18*, 1463–1472.
- (37) Berendsen, H. J. C.; Postma, J. P. M.; Gunsteren, W. F.; Dinola, A.; Haak, J. R. Molecular dynamics with coupling to an external bath. *J. Chem. Phys.* **1984**, *81*, 3684–3689.
- (38) Feenstra, K. A.; Hess, B.; Berendsen, H. J. C. Improving efficiency of large time-scale molecular dynamics simulations of hydrogen-rich systems. *J. Comput. Chem.* **1999**, *20*, 786–798.
- (39) Colombo, G.; Marrink, S.; Mark, A. E. Simulation of mscl gating in a bilayer under stress. *Biophys. J.* **2003**, *84*, 2331–2337.
- (40) Bandyopadhyay, S.; Chanda, J. Monolayer of monododecyl diethylene glycol surfactants adsorbed at the air/water interface: a molecular dynamics study. *Langmuir* **2003**, *19*, 10443–10448.
- (41) Marrink, S. J.; Lindahl, E.; Edholm, O.; Mark, A. E. Simulation of the spontaneous aggregation of phospholipids into bilayers. *J. Am. Chem. Soc.* **2001**, *123*, 8638–8639.
- (42) Marrink, S. J.; Tieleman, D. P. Molecular dynamics simulation of spontaneous membrane fusion during a cubic-hexagonal phase transition. *Biophys. J.* **2003**, *83*, 2386–2392.

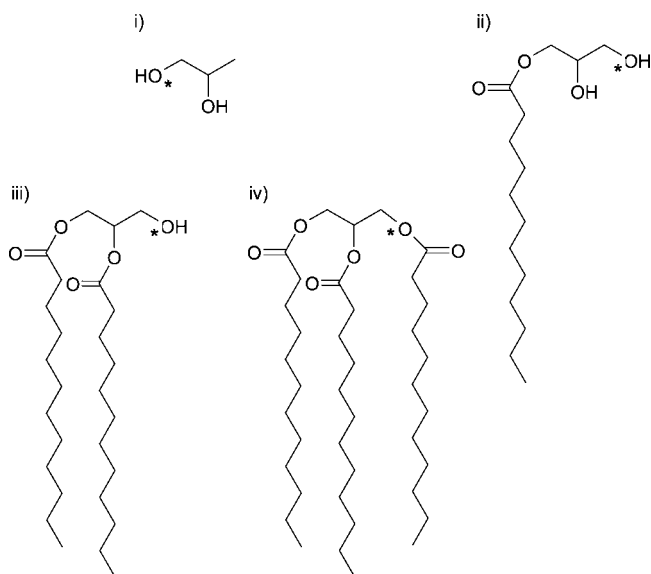


Figure 1. Structure of molecules simulated: (i) propylene glycol (PG), (ii) monooleoyl glyceride (MGL), (iii) dioleoyl glyceride (DGL), and (iv) triooleoyl glyceride (TGL). An asterisk marks the O3 atom of each molecule.

Table 1. Specifications for the Propylene Glycol (PG) and Water Systems Studied

	PG		water	
	number	% w/w (% mol)	number	% w/w (% mol)
single PG in water	1	0.025 (0.006)	17,131	99.975 (99.994)
1% w/w PG with water	45	1.085 (0.259)	17,325	98.915 (99.741)
5% w/w PG with water	230	5.407 (1.335)	16,994	94.593 (98.665)
20% w/w PG with water	1,030	21.354 (6.040)	16,022	78.646 (93.960)
50% w/w PG with water	2,800	52.063 (20.454)	10,889	47.937 (79.546)
80% w/w PG with water	4,500	81.289 (50.704)	4,375	18.711 (49.296)
95% w/w PG with water	5,500	95.377 (83.006)	1,126	4.623 (16.994)
99% w/w PG with water	6,000	99.077 (96.216)	236	0.923 (3.784)
100% w/w	4,488	100.000 (100.000)	0	0.000 (0.000)

around the average values. Simulations were run for a total simulation time of 40 ns, unless otherwise noted.

Simulated Systems. The five molecules used in the simulations were propylene glycol (PG), monooleoyl glyceride (MGL), dioleoyl glyceride (DGL), triooleoyl glyceride (TGL) and water (SOL), with their molecular structures shown in Figure 1. The systems studied comprised PG with increasing water content, see Table 1; MGL and DGL in 1:1 mass and molar ratios with increasing water content, see Table 2; MGL, DGL, PG and water, see Table 3; and MGL, DGL and TGL in 1:1:1 mass ratio with increasing water content, see Table 4.

Parametrization of Propylene Glycol. The 43a2 united atom forcefield utilized for this study contained no parameters to deal with PG, therefore the appropriate parameters were

developed. The parameters for an alcohol functional group taken from the 43a2 forcefield were used as the starting point, followed by an iterative parameter fitting process. The forcefield parameters were adjusted to fit the experimental density and latent heat of vaporization (ΔH_{vap}) of PG with the same physical properties obtained from the MD simulations. The MD ΔH_{vap} was calculated using eq 1. The $E_{\text{intra}}(\text{g})$ term is obtained from the potential energy of a single PG molecule in vacuum and $E_{\text{intra}}(\text{liq})$ from the potential energy of pure PG.

$$\Delta H_{\text{vap}} = [E_{\text{intra}}(\text{g}) + RT] - [E_{\text{intra}}(\text{liq}) + E_{\text{inter}}(\text{liq})] \quad (1)$$

where $E_{\text{intra}}(\text{g})$ is the intramolecular energy of the gas phase (J mol^{-1}), R is the gas constant ($\text{J K}^{-1} \text{mol}^{-1}$), T is the temperature (K), $E_{\text{intra}}(\text{liq})$ is the intramolecular energy of the liquid phase, and $E_{\text{inter}}(\text{liq})$ is the intermolecular energy of the liquid phase (J mol^{-1}).

Results

Parametrization of Propylene Glycol. The 43a2 united atom forcefield parameters that provided the best fit of the experimental PG physical properties are presented in Table 5, and a comparison between the experimental and MD physical properties is presented in Table 6. These partial charges have also been used by Zhao et. al⁴³ for the partial charges of the atoms within the glycol group of palmitoyl-oleoylphosphatidylglycerol.

Pure Components. The glycerides (MGL, DGL and TGL) and PG were simulated as pure components to obtain structural information, see Figure 2, and physical properties, see Table 7. Both PG and TGL form continuous phases without any significant structuring present, see Figure 2i and Figure 2iv, respectively. This is expected for PG, due to the molecule's small size and relative ease of molecular rotation. TGL lacks any structuring of the molecules as the ester groups it contains do not have hydrogen bond donors to allow any intermolecular bonding. Additionally, the ester groups are well shielded from adjacent molecules by the three nonyl chains. Conversely, MGL forms a dynamic "bicontinuous phase"-like structure, see Figure 2ii. This consists of a three-dimensional networked region containing the hydrogen bonded $-\text{OH}$ surrounded by the nonyl chains. DGL also exhibits a significant amount of interaction between the $-\text{OH}$ group of the DGL headgroup, see Figure 2iii. However, it is more reverse micellar-like in character, forming dynamic clusters of 4 to 8 interacting head groups surrounded by the nonyl chains. The densities calculated from these simulations are consistent with those determined experimentally; see

(43) Zhao, W.; Rog, T.; Gurtovenko, A. A.; Vattulainen, I.; Karttunen, M. Atomic-scale structure and electrostatics of anionic palmitoyl-oleoylphosphatidylglycerol lipid bilayers with Na^+ counterions. *Biophys. J.* **2007**, *92*, 1114–1124.

(44) Dean, J. A. *Lange's handbook of chemistry*; McGraw-Hill: Sydney, 1999.

Table 2. Specifications for the Mono-Lauroyl Glyceride (MGL), Di-Lauroyl Glyceride (DGL) and Water Systems Studied

	MGL		DGL		SOL	
	number	% w/w (% mol)	number	% w/w (% mol)	number	% w/w (% mol)
1:1 molar ratio MGL:DGL	110	37.532 (50.000)	110	62.468 (50.000)	0	0 (0)
1:1 molar ratio MGL:DGL with						
1% w/w water	600	37.157 (41.494)	600	61.843 (41.494)	246	1.000 (17.012)
5% w/w water	600	35.654 (24.164)	600	59.341 (24.164)	1,283	5.005 (51.671)
10% w/w water	600	33.776 (15.353)	600	56.216 (15.353)	2,708	10.008 (69.294)
15% w/w water	600	31.898 (10.907)	600	53.090 (10.907)	4,301	15.012 (78.186)
20% w/w water	600	30.020 (8.227)	600	49.965 (8.227)	6,093	20.015 (83.546)

Table 3. Specifications for the Mono-Lauroyl Glyceride (MGL), Di-Lauroyl Glyceride (DGL), Propylene Glycol (PG) and Water Systems Studied

	MGL		DGL		PG		SOL	
	number	% w/w (% mol)	number	% w/w (% mol)	number	% w/w (% mol)	number	% w/w (% mol)
1:1 molar ratio MGL:DGL with								
18% w/w PG and 10% w/w water	500	27.021 (9.575)	500	44.973 (9.752)	1,306	18.005 (25.473)	2,821	10.008 (55.022)
16% w/w PG and 20% w/w water	500	24.019 (5.778)	500	39.976 (5.778)	3,133	16.004 (15.093)	6,347	20.000 (73.350)
45% w/w PG and 10% w/w water	300	16.890 (4.658)	300	28.112 (4.658)	1,306	44.998 (48.642)	2,708	10.000 (42.043)
40% w/w PG and 20% w/w water	300	15.011 (3.053)	300	24.984 (3.053)	3,133	39.992 (31.888)	6,092	20.013 (62.005)

Table 4. Specifications for the Mono-Lauroyl Glyceride (MGL), Di-Lauroyl Glyceride (DGL), Tri-Lauroyl Glyceride (TGL) and Water Systems Studied

	MGL		DGL		TGL		water	
	number	% w/w (% mol)	number	% w/w (% mol)	number	% w/w (% mol)	number	% w/w (% mol)
1:1:1 mass ratio MGL:DGL:TGL with								
1% w/w water	1,164	32.986 (40.110)	700	33.016 (24.121)	500	32.997 (17.229)	538	1.001 (18.539)
5% w/w water	1,164	31.656 (22.554)	700	31.684 (13.563)	500	31.666 (9.688)	2,797	4.995 (54.195)
10% w/w water	1,164	29.981 (14.043)	700	30.008 (8.445)	500	29.991 (6.032)	5,925	10.019 (71.480)
15% w/w water	1,164	28.281 (9.828)	700	28.307 (5.910)	500	28.290 (4.222)	9,480	15.122 (80.041)
20% w/w water	1,164	26.685 (7.465)	700	26.709 (4.489)	500	26.694 (3.207)	13,229	19.912 (84.839)
1:1:2 mass ratio MGL:DGL:TGL with 1% w/w water	873	24.740 (32.502)	525	24.763 (19.549)	750	49.496 (27.923)	538	1.001 (20.030)

Table 5. Derived 43a2 Forcefield Parameters for Propylene Glycol

atom	partial charge, q (e)	Lennard-Jones interaction parameters	
		C^6 (kJ mol ⁻¹ nm ⁶)	C^{12} (kJ mol ⁻¹ nm ¹²)
CH ₃	0.000	0.0084536880	3.406966×10^{-5}
CH ₂	+0.157	0.0071048041	2.5775929×10^{-5}
CH	+0.157	0.0037797904	1.1377129×10^{-5}
O	-0.574	0.0019765575	1.875140×10^{-6}
H	+0.417	0	0

Table 7, once the difference in measurement temperatures are taken into consideration. van Buuren et al.⁴⁵ previously performed simulations of DGL at 27 °C, using a united atom forcefield, and calculated a density of 980 kg m⁻³ and

(45) van Buuren, A. R.; de Vlieg, J.; Berendsen, H. J. C. Structural properties of 1,2-diacyl-sn-glycerol in bulk and at the water interface by molecular dynamics. *Langmuir* **1995**, *11*, 2957–2965.

Table 6. Comparison of Experimental⁴⁴ and Simulated Physical Properties of Propylene Glycol

	exptl ⁴⁴	this study
density at 293 K (kg m ⁻³)	1036.4	1035
ΔH_{vap} at 298 K (kJ mol ⁻¹)	58.0	56.7
dipole moment	2.27	2.59

diffusion coefficient of 7.4×10^{-7} cm² s⁻¹, which are consistent with the values obtained in this study.

Propylene Glycol and Water. The structural behavior of PG with the addition of water is shown in Figure 3, from 0 to 99% w/w water. Pure propylene glycol exhibits no significant microstructuring, forming a continuous phase, see Figure 3i. With the addition of a small amount of water, 1% w/w, the water fully disperses through the PG phase, see

(46) Lide, D. R. *CRC handbook of chemistry and physics: a ready reference book of chemical and physical data*; CRC Press: Boca Raton, 1999.

(47) ACD/Labs, Advanced chemistry development software, 8.14, 2008.

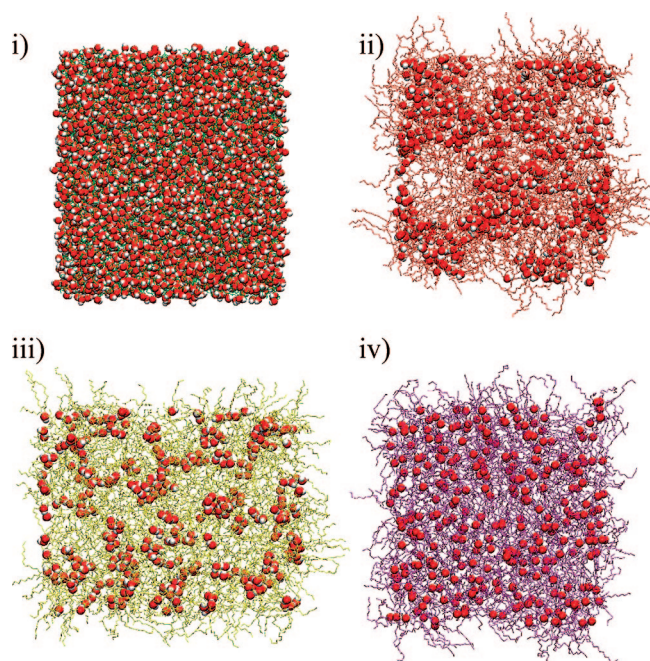


Figure 2. Structure of (i) PG, (ii) MGL, (iii) DGL, and (iv) TGL pure component systems. Molecules are represented as lines, with molecule coloring of green, PG; red, MGL; yellow, DGL; and purple, TGL. Atom coloring is red, O3; and white, H3.

Table 7. Properties of Pure Component Systems Obtained via Molecular Dynamics Simulations and Comparison with Experimental Results

	density		diffusion constant
	exptl (kg m ⁻³)	this study at 37 °C (kg m ⁻³)	this study × 10 ⁷ (cm ² s)
PG	1,036.4 ⁴⁴ at 44 °C	1,029	0.70
MGL	924.8 ⁴⁶ at 97 °C	1,038	1.05
DGL	953 ⁴⁷ at 20 °C	995	1.83
TGL	898.5 ⁴⁶ at 55 °C	981	2.57

Figure 3ii. When it is increased to 5% w/w water, small clustering of some water molecules occurs, but the majority is still fully dispersed through the PG-rich phase, see Figure 3iii. Once 20% w/w water is reached, a phase change or separation has occurred, with large water pools being formed, see Figure 3iv. However, some water molecules are still dispersed through the PG-rich phase and visa versa for PG in the water-rich phase. For the case of 50% w/w water, two distinct water-rich and PG-rich layers are formed, again with some of each component dispersed through the other's rich phase, see Figure 3v. At 80% w/w water, the situation is a reversal of the 20% w/w water case, see Figure 3vi. A phase which is PG rich is present within a continuous water-rich phase. Once 95% w/w water is reached, PG is now fully dispersed within the water-rich phase, with only limited clustering of PG molecules occurring, see Figure 3vii. And finally, at 99% w/w water, it is a reversal of the 1% w/w water situation, with PG fully dispersed through the water phase.

The percentage hydration of water and PG molecules was calculated, with the results shown in Figure 4 for the first hydration shell. The second and third hydration shells for both molecules exhibit the same behavior. The dramatic increase in the hydration of water from 1 to 20% w/w water is consistent with that observed visually in Figure 3. By 50% w/w water, the majority of the water is present in an environment that is approaching that of unconstrained, bulk water. A similar dramatic increase in the percentage hydration of PG is observed from 80 to 95% w/w water, indicating that up until this point the majority of PG is associated with other PG molecules. Once the system reaches the 80% w/w water point, then there is sufficient water such that majority of the PG molecules start to approach that of a fully hydrated molecule. The same behavior of the system is also observed by calculating the diffusion coefficient, see Figure 5. A dramatic increase in the diffusion coefficient for water is observed at the next composition step, from 20 to 50% w/w water. A similar increase is observed for PG from 80 to 95% w/w water. The higher diffusion coefficient of PG solvated in water versus pure PG is a result of the constrained rotation and motion from the different molecule shapes and additional hydrophobic interactions that occur between PG–PG molecules. The percentage hydration and diffusion coefficients both provide a suitable numerical indicator on the state of the molecules to bulk or fully solvated in water.

It is widely known that propylene glycol is fully miscible in water.⁴⁶ It appears from this study that even though it is fully miscible with water, there may be some microstructuring of the phase that is formed by mixing these two solvents. Care must be taken in the interpretation of these results, as the structuring observed could be an artifact of the forcefield parametrization for the PG molecule. As confirmation of this structuring observed, a mention has been made by Nagami and Kato⁴⁸ in an experimental study using polarographic examination of the diffusion coefficient of oxygen in propylene glycol/water systems, that around the 50% composition, some sudden change in the internal structure takes place. The microstructuring of PG–water mixtures is worthy of further investigation but was not our primary objective, and therefore we did not investigate this effect experimentally as part of this study.

Mono- and Di-Lauroyl Glyceride and Water. The spontaneous structuring of two MGL/DGL systems with water is shown in Figure 6 to illustrate how the systems evolve with simulation time. For all the glyceride systems studied, it was found that within 1 ns all the molecules have aggregated into reverse micelles, with the glycerol backbone of the glycerides arranged to allow hydrogen bonding with each other and water molecules. After 15 ns of simulation time, these structures had evolved into a dynamically stable state, with no major structural/conformational changes occurring.

(48) Nogami, H.; Kato, Y. Diffusion coefficient of oxygen in propylene glyco-water mixtures and glycerol-water mixtures. *Yakugaku Zasshi* **1962**, *82*, 120–126.

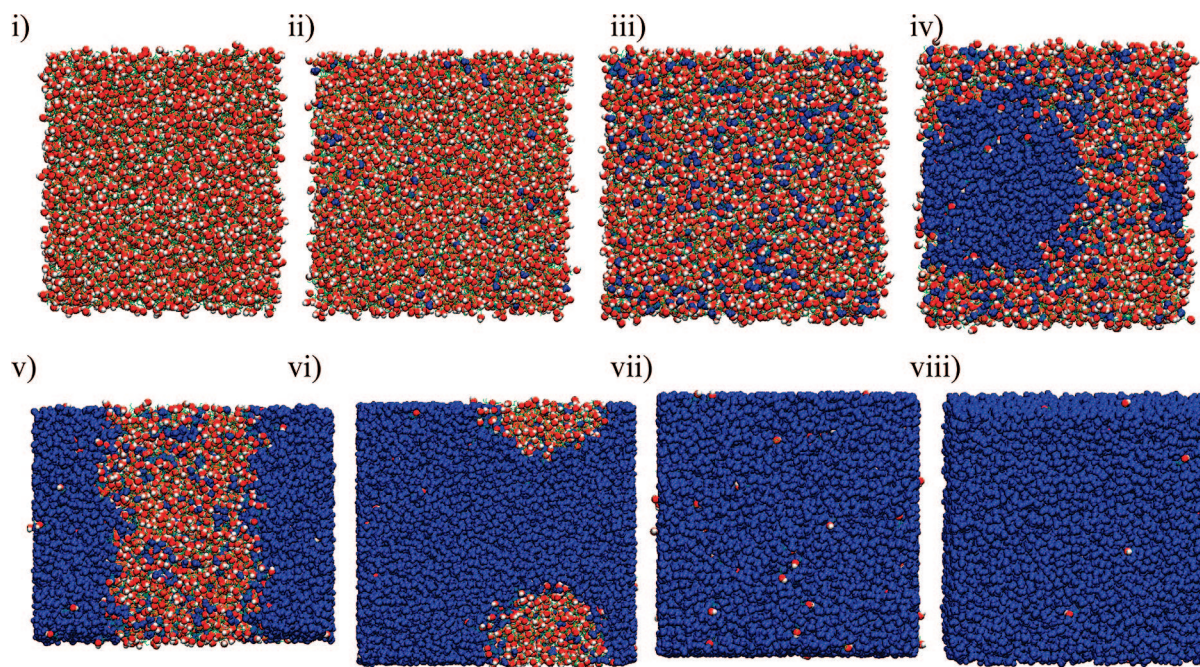


Figure 3. Structure of PG systems with increasing water content (% w/w): (i) 0, (ii) 1, (iii) 5, (iv) 20, (v) 50, (vi) 80, (vii) 95, and (viii) 99. Molecule coloring is blue, water; and green, PG. Atom coloring is red, O3 of PG; and white, H3 of PG.

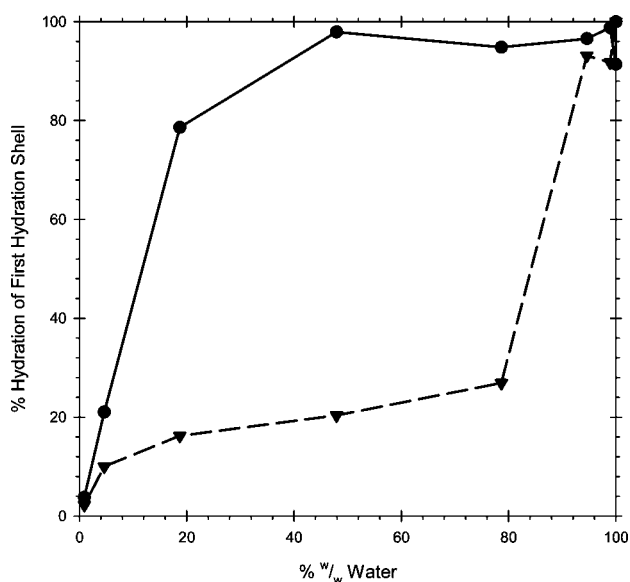


Figure 4. Effect of % w/w water content on the percentage hydration of the first hydration shell around the O3 atom of PG (▼) and the water oxygen atom (●).

The effect of water content on the structures formed at the conclusion of the simulations is shown in Figure 7. When no water is present, the glycerol backbones of both MGL and DGL hydrogen bond, forming reverse micellar-like structures with the hydrophilic region forming a cigar shape, see Figure 7i. When trace water is added (1% w/w water), these water molecules hydrogen bond with the glyceride –OH and ester groups, see Figure 7ii. The addition of further water (5% w/w water) swells these reverse micelles, making them more spherical, see Figure 7iii. Subsequent increases in the water content (10, 15 and 20% w/w water) swells these

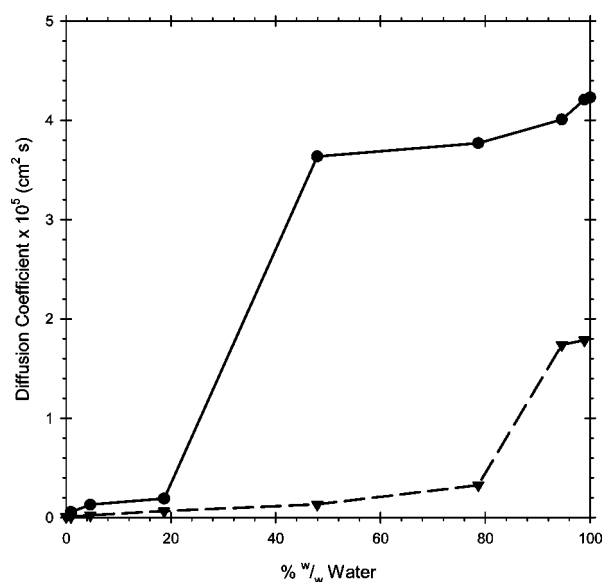


Figure 5. Effect of % w/w water content on the diffusion coefficient of PG (▼) and water (●).

reverse micelles, see Figure 7iv, Figure 7v and Figure 7vi, respectively.

The ordering of the glyceride nonyl chains was monitored using the trans-dihedral fraction. Across the entire range studied (1–20% w/w water) there was only a very minor increase in the trans fraction, from 76.6 to 77.8%. Nevertheless, this change was a constant linear increase with the increasing water content.

The percentage hydration of MGL, DGL and water molecules was calculated and is shown in Figure 8 for the first hydration shell (with the second and third shells exhibiting the same behavior). The most dramatic change

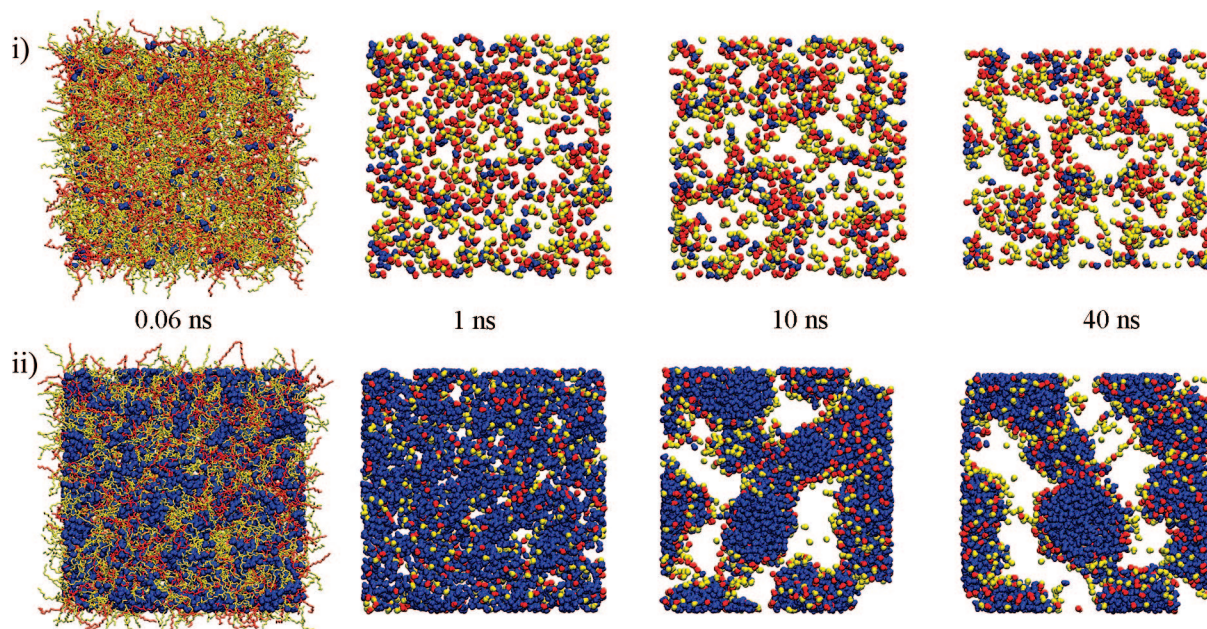


Figure 6. The spontaneous structuring of 1:1 molar ratio MGL:DGL systems with SOL over a 40 ns simulation: (i) 1% w/w and (ii) 15% w/w water. Molecule coloring is blue, water. Atom coloring is red, O3 and H3 of MGL; yellow, O3 and H3 of DGL; and purple, O3 of TGL. Alkyl chains of glycerides after first image omitted for clarity.

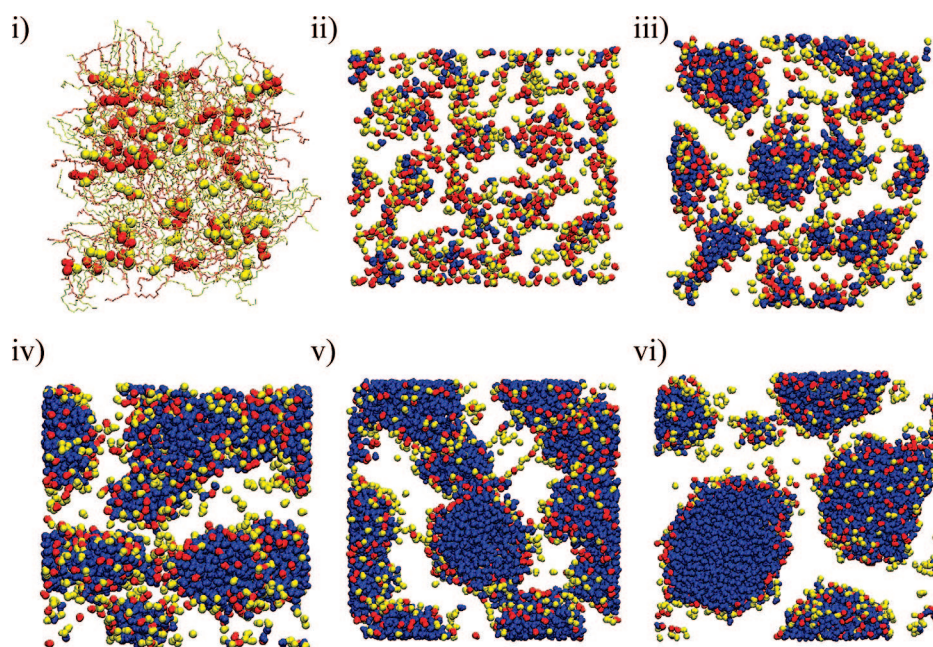


Figure 7. Structure of MGL:DGL (1:1% mol) system with increasing water content (% w/w): (i) 0, (ii) 1, (iii) 5, (iv) 10, (v) 15, and (vi) 20. Molecule coloring is blue, water. Atom coloring is red, O3 and H3 of MGL; and yellow, O3 and H3 of DGL. Alkyl chains of glycerides after first image omitted for clarity.

in the hydration of the molecules is in the first 5% w/w addition of water, when the size of the water aggregates is such that there can be more than just a couple of water molecules involved. The same behavior of the system is observed with the diffusion coefficient, results not shown.

Mono-, Di-, and Tri-Lauroyl Glyceride and Water. The organization and dynamics of the resulting structures for various compositions with MGL, DGL, and TGL were analyzed, including the influence of increasing water concentration.

The water composition for a 1:1:1 MGL:DGL:TGL weight ratio system was varied from 0 to 20% w/w in five simulations. Each formulation was found to form reverse micellar-like structures (water pools bounded by hydrophilic glyceride head groups and surrounded by alkyl chain regions), see Figure 9. Reverse micelle-like structures form even in the absence of water. Increasing the water content causes the spherical water pools to swell and changed the molecular distributions. At low water contents, both MGL and DGL form the reverse micelles, interacting via hydrogen

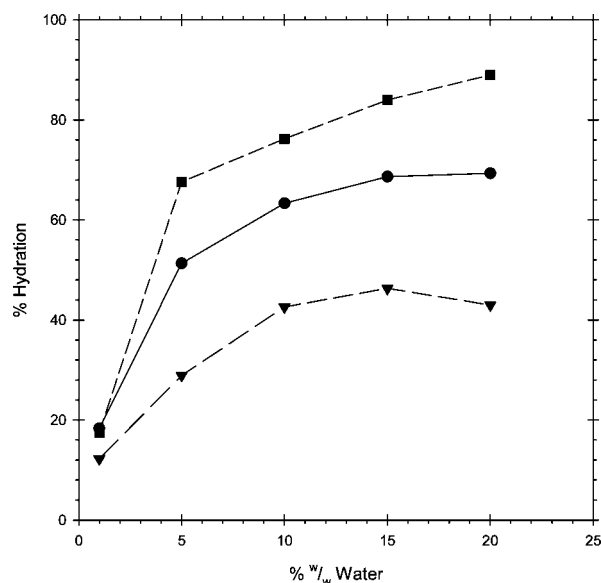


Figure 8. Effect of % w/w water content on the percentage hydration of the first hydration shell around the O3 atom of MGL (●) and DGL (▼), and the oxygen of water (■).

bonding with each other and the water molecules. The hydrophilic regions of the micelles are not spherical but prolate and are also dynamic in nature. When 5% w/w water is reached, the aggregates are more stable and become more spherical in nature. After this point, adding further water simply increases the size of the water pools, with the head groups of MGL and DGL arranged on the surface, allowing strong hydrogen bonding/hydration of the functional groups. TGL is present within the hydrophobic space in between, with the glyceride head groups dispersed evenly within these alkyl dominated regions.

These simulations indicate that these types of lipid formulations exhibit microstructuring, even though they appear to be homogeneous on the macroscopic scale. Initial analysis shows that these systems have a larger hydrophobic phase than a similar system containing just MGL and DGL (1:1 mass ratio). This may be an advantage for more hydrophobic drugs. The impact that this has on drug solubility and subsequent dispersion/digestion within the intestinal tract will be explored and has not previously been considered. If the TGL relative content is doubled, then the system is structurally the same with a larger hydrophobic region, results not shown. The same behavior of the diffusion coefficient and percentage water hydration is observed as for the MGL/DGL system.

Propylene Glycol, Mono- and Di-Lauroyl Glyceride and Water. MGL and DGL with differing amounts of PG and water were simulated, with the phase structures formed shown in Figure 10. All systems formed a 3D network heterogeneous phase structure, with hydrophobic regions containing the glyceride alkyl chains surrounded by the hydrophilic head groups and solvents. Due to the limitations in the scale of these simulations, it is unclear what the exact nature of these structures are; they may be an artifact of the

simulation size. The diffusion coefficients of MGL and DGL were unchanged for all four systems ($3 \times 10^{-7} \text{ cm}^2 \text{ s}^{-1}$). For the systems with 10% w/w water, increasing the amount of PG, see Figure 10i and Figure 10iii, makes the system more homogeneous, spreading out and breaking up the water pools that form. This is evident visually and by the effect on the water diffusion coefficient, increasing from 7.42 to $19.0 \times 10^{-7} \text{ cm}^2 \text{ s}^{-1}$. This increase is due to the water being replaced in interacting with the glyceride $-\text{OH}$ groups being displaced by PG which undergoes a corresponding decrease in diffusion coefficient from 7.64 to $6.45 \times 10^{-7} \text{ cm}^2 \text{ s}^{-1}$. For the systems with 20% w/w water, adding more PG, see Figure 10ii and Figure 10iv, similar behavior is observed with the water diffusion coefficient increasing from 24.5 to $31.3 \times 10^{-7} \text{ cm}^2 \text{ s}^{-1}$ and PG decreasing from 12.3 to $7.34 \times 10^{-7} \text{ cm}^2 \text{ s}^{-1}$. For the systems with the low PG composition, increasing the water content (which corresponds to the dilution process that occurs when taken orally) causes the water pools to increase in size with a corresponding increase in the diffusion coefficient of water from 7.42 to $24.5 \times 10^{-7} \text{ cm}^2 \text{ s}^{-1}$. No change in the degree of hydration of MGL and DGL occurs, indicating also that the added water is simply increasing the size of the water pools. The same behavior is observed when the water content is increased at the high PG composition, the water diffusion coefficient increasing from 19.0 to $31.1 \times 10^{-7} \text{ cm}^2 \text{ s}^{-1}$.

Discussion

Capsule formulations of poorly water-soluble drugs are becoming increasingly popular as a means of maximizing bioavailability from the gastrointestinal tract. A variety of excipients can be used in capsule formulations ranging from water-miscible materials to oils with very limited aqueous solubility.⁹ The microstructure of such formulations is difficult to study by physical methods due to the polymeric nature of many of the excipients. MD offers an alternative method to gain insight into microstructure and is beginning to attract the attention of pharmaceutical scientists.^{49,50} Simple oil formulations, typically comprising mixed glycerides, which we refer to as type I,⁹ have been used to formulate a number of lipophilic drugs.⁵¹ Several excipient manufacturers supply mixtures of medium-chain mono- and diglycerides derived from coconut oil,⁵² that are well

(49) Xiang, T. X.; Jiang, Z. Q.; Song, L.; Anderson, B. D. Molecular dynamics simulations and experimental studies of binding and mobility of 7-tert-butylidimethylsilyl-10-hydroxycamptothecin and its 20(s)-4-aminobutyrate ester in dmpc membranes. *Mol. Pharmaceutics* **2006**, *3*, 589–600.

(50) Rane, S. S.; Anderson, B. D. Molecular dynamics simulations of functional group effects on solvation thermodynamics of model solutes in decane and tricaprolin. *Mol. Pharmaceutics* **2008**, *5*, 1023–1036.

(51) Strickley, R. D. Currently marketed oral lipid-based dosage forms: drugs products and excipients. In *Oral lipid-based formulations: enhancing the bioavailability of poorly water soluble drugs*; Hauss, D. J., Ed.; Informa Healthcare Inc.: New York, 2007; pp 1–31.

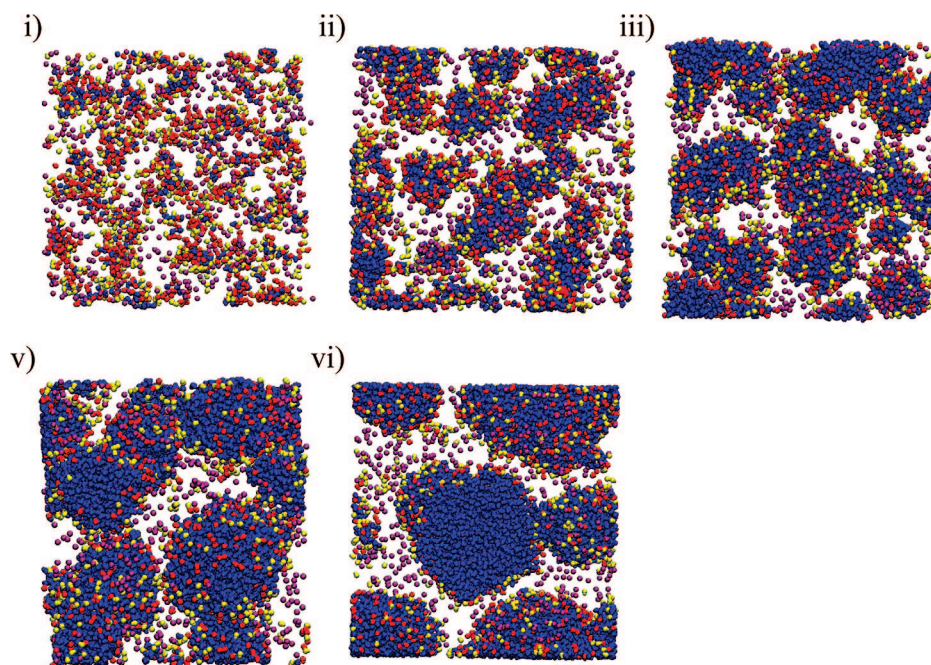


Figure 9. Structure of MGL:DGL:TGL (1:1:1% w/w) system with increasing water content (% w/w): (i) 1, (ii) 5, (iii) 10, (iv) 15, and (v) 20. Molecule coloring is blue, water. Atom coloring is red, O3 and H3 of MGL; yellow, O3 and H3 of DGL; and purple, O3 of TGL. Alkyl chains of glycerides omitted for clarity.

tolerated food and pharmaceutical materials, not encumbered by regulatory concerns. These are often used alone or in combination with triglycerides. Glycerol monooleate (which usually contains dioleates) is another well tolerated excipient derived from vegetable oils. Mixed glycerides are generally better solvents than triglycerides for many drugs, and have the added advantage that they blend well with surfactants and cosolvents. Thus self-emulsifying formulations often contain mixed glycerides where they act as cosolvent, enhancing the uptake of water and promoting emulsification.^{8,9} In this study we focus on the changes which occur in the microstructure of mixed glycerides as they take up water, in the presence or absence of triglycerides, and have focused on the lauroyl (C12) esters in the first instance. The uptake of water into formulations is an inevitable consequence of the release of the gelatin capsule contents into the stomach, and is likely to result in phase separation and possible precipitation of drug. Since lipid-based formulations perform much better when the drug is maintained in solution, we regard this as a good starting point to explore the value of MD simulations of lipid-based formulations. Cosolvents, such as polyethylene glycol or PG, are also used in lipid formulations and can be blended with mixed glycerides to produce surfactant-free formulations which are better solvents for drugs that dissolve well in cosolvents. For this reason we also explored the aqueous dilution of pure PG and the microstructure of blends of PG with mixed glycerides as they take up water. Blending cosolvents with mixed glycerides

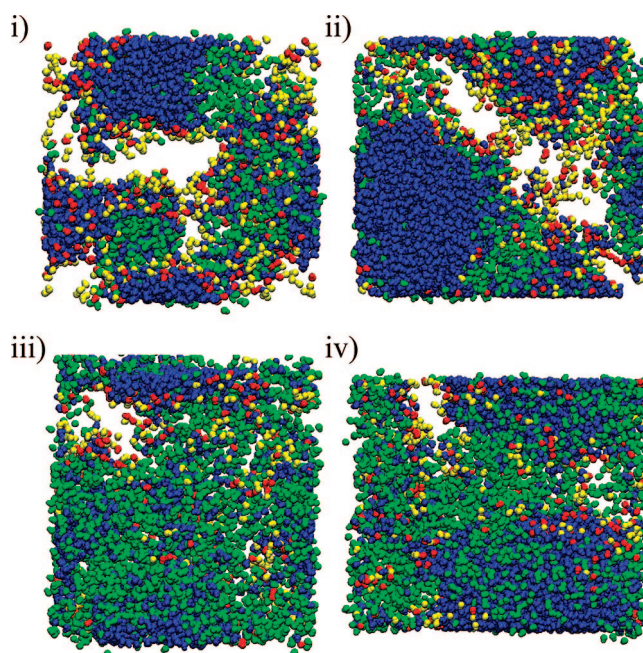


Figure 10. Structure of MGL, DGL and PG systems with increasing water content: (i) 10% w/w water and 18% w/w PG, (ii) 20% w/w water and 16% w/w PG, (iii) 10% w/w water and 45% w/w PG, and (iv) 20% w/w water and 40% w/w PG. Molecule coloring is blue, water. Atom coloring is red, O3 and H3 of MGL; yellow, O3 and H3 of DGL; and green, O3 and H3 of PG.

can reduce the incident of precipitation, hence our interest in properties of these formulations.

Establishment of the forcefield parameters for propylene glycol was successful as shown in Table 6, achieving satisfactory correlation between experimental and simulated

(52) Gibson, L. Lipid-based excipients for oral drug-delivery. In *Oral lipid-based formulations: enhancing the bioavailability of poorly water soluble drugs*; Hauss, D. J., Ed.; Informa Healthcare Inc.: New York, 2007; pp 33–61.

physical properties of PG. We intend to go forward to model formulations including nonionic (ethoxylated) surfactants using MD, which requires parametrization of the ethoxy chain for the GROMOS united-atom forcefield. One issue with modeling surfactants is that as yet we do not have literature values of density, ΔH_{vap} or dipole moment for typical pharmaceutical surfactants. These experimental measurements may need to be made to improve parametrization in the future.

MD simulations of two-component mixtures of PG and water revealed that there is considerable association between PG molecules until the water content rises beyond 80% w/w, when PG begins to become fully solvated. It will be interesting to test how this phenomenon is modified in the presence of druglike molecules. We did not pursue PG–water mixtures any further in this study because they are not very useful formulations for poorly water-soluble drugs.

MD simulations of the mixed glyceride formulations and mixed glyceride/PG formulations clearly identified association structures within the formulations and predicted phase separation of formulations on dilution with water. The calculation of the percentage hydration (Figure 8) was an effective way to compare the environments of the glycerides at different water contents. PG clearly promoted the adsorption of water as exemplified in Figure 10. At high water contents in each case, pools of free water are observed. This represents the existence of a separate aqueous phase into which it is speculated that a formulated drug is likely to partition, depending on its physicochemical properties. We expect that this type of MD simulation will allow us to predict the location of drug molecules during dispersion of

the formulation. This will indicate whether a formulation is likely to prevent precipitation or not and possibly allow optimization of formulation to minimize precipitation.

Summary and Conclusions

The microstructure of type I lipid formulations consisting of mixed glycerides (monolauroyl glyceride (MGL) and dilauroyl glyceride (DGL)) has been investigated using molecular dynamics simulations. We have investigated the anhydrous formulations and those containing trace amounts of water, which represents the expected water content of a blend of glyceride excipients in a soft-gelatin capsule. All the systems (MGL/DGL, MGL/DGL and PGO, and MGL/DGL/TGL) investigated exhibited microstructural features representative of reverse micelles. Each formulation consists of distinct regions of hydrophobic and hydrophilic character. These systems were then investigated with increasing proportions of water, providing an insight into how the structure changes with dispersion of the formulation in an aqueous phase. MD modeling shows great potential as a predictive tool for the structure of lipid formulations, and subsequent studies based on this preliminary work will explore the predictive potential to identify suitable lipid formulations for drugs prone to precipitation on dilution or dispersion of the formulation.

Acknowledgment. Financial support from Cardinal Health is gratefully acknowledged. We would also like to thank the Australian Partnership for Advanced Computing (APAC) for the Merit Allocation Scheme grant.

MP8001667